Cerebral Cortex February 2014;24:444–451
doi:10.1093/cercor/bhs321
Advance Access publication October 18, 2012

Number–Space Interactions in the Human Parietal Cortex: Enlightening the SNARC Effect with Functional Near-Infrared Spectroscopy

Simone Cutini[1], Fabio Scarpa[2], Pietro Scatturin[2], Roberto Dell'Acqua[2,3] and Marco Zorzi[1,3]

[1]Department of General Psychology, University of Padova, Venice 35131, Italy, [2]Department of Developmental Psychology and Socialization, University of Padova, Venice 35131, Italy and [3]Center for Cognitive Science, University of Padova, Venice 35131, Italy

Address correspondence to Prof. Marco Zorzi, Department of General Psychology, University of Padova, Via Venezia 8, Venice 35131, Italy. Email: marco.zorzi@unipd.it

Interactions between numbers and space have become a major issue in cognitive neuroscience, because they suggest that numerical representations might be deeply rooted in cortical networks that also subserve spatial cognition. The spatial–numerical association of response codes (SNARC) is the most robust and widely replicated demonstration of the link between numbers and space: in magnitude comparison or parity judgments, participants' reaction times to small numbers are faster with left than right effectors, whereas the converse is found for large numbers. However, despite the massive body of research on number–space interactions, the nature of the SNARC effect remains controversial and no study to date has identified its hemodynamic correlates. Using functional near-infrared spectroscopy, we found a hemodynamic signature of the SNARC effect in the bilateral intraparietal sulcus, a core region for numerical magnitude representation, and left angular gyrus (ANG), a region implicated in verbal number processing. Activation of intraparietal sulcus was also modulated by numerical distance. Our findings point to number semantics as cognitive locus of number–space interactions, thereby revealing the intrinsic spatial nature of numerical magnitude representation. Moreover, the involvement of left ANG is consistent with the mediating role of verbal/cultural factors in shaping interactions between numbers and space.

Keywords: functional near-infrared spectroscopy, functional neuroimaging, number–space interactions, numerical cognition, SNARC effect

Introduction

Interactions between numbers and space have become a major issue in cognitive neuroscience, because they suggest that numerical representations might be deeply rooted in cortical networks that also subserve spatial cognition (Zorzi et al. 2002; Hubbard et al. 2005). The most robust and widely replicated phenomenon suggesting a link between numbers and space is the spatial–numerical association of response codes (SNARC) effect (Dehaene et al. 1993). In magnitude comparison or parity judgments, participants' reaction times (RTs) to small numbers are faster with left than right effectors, whereas the converse is found for large numbers. This effect is remarkably flexible, because what is left and what is right depends on the range of numerical stimuli (i.e., small and large is relative rather than absolute; Dehaene et al. 1993; Fias et al. 1996) and on cultural factors such as reading habits (Shaki et al. 2009; Gobel et al. 2011). Nevertheless, the dominant view is that the SNARC effect taps the spatial nature of a semantic representation of number magnitude, that is, a mental number line that, in Western cultures, is oriented from left to right (Zorzi et al. 2002; Dehaene et al. 2003; Hubbard et al. 2005; Nuerk et al. 2005; Castronovo and Seron 2007; Zorzi et al. 2012).

This view has been recently challenged by alternative accounts that either dispense with the spatial coding hypothesis or maintain that number–space interaction has predominantly a verbal–conceptual (rather than visuospatial) origin (Fias et al. 2011). Building on electrophysiological findings suggesting that the SNARC effect originates at a response-related processing stage (Keus and Schwarz 2005; Keus et al. 2005; Gevers, Ratinckx, et al. 2006), a recent computational account (Gevers, Verguts, et al. 2006) assumes that the effect is the result of response competition due to the automatic activation of left/right responses associated with the conceptual coding of numbers as small/large. Thus, this hypothesis maintains that there is nothing intrinsically spatial in the mental representation of numbers (Proctor and Cho 2006). In addition to the controversy surrounding the cognitive locus of the SNARC effect (Gevers and Lammertyn 2005), no study to date has identified its hemodynamic correlates. This is at odds with the extensive behavioral investigation of this phenomenon (and of number–space interactions, more generally), and it is in sharp contrast with the remarkable progress during the recent years in understanding the neural basis of numerical cognition.

A large body of neuroimaging and neuropsychological studies, as well as neurophysiological findings on nonhuman primates, converge in indicating the parietal cortex as the region that contains the core cortical circuits for number processing (Dehaene et al. 2003; Hubbard et al. 2005). In particular, it is widely believed that the horizontal portion of the intraparietal sulcus (hIPS) is the neural substrate of a supramodal, language-independent representation of numerical magnitude (Eger et al. 2003; Piazza et al. 2004; Zorzi et al. 2011). This region responds to numerical information irrespective of stimulus format (e.g., Arabic numbers, number words, dot patterns) (Eger et al. 2003; Piazza et al. 2004, 2007) and is consistently active during magnitude comparison and mental calculation (Chochon et al. 1999; Pinel et al. 2001), even across cultures (Tang et al. 2006). Besides hIPS, 2 other parietal regions play a key role in numerical cognition, as suggested by an influential meta-analysis (Dehaene et al. 2003): the bilateral posterior portion of the superior parietal lobe, which is involved in attentional processes but is not specific to the number domain, and the left angular gyrus (ANG), which is associated with verbal number representation and other linguistic aspects of number processing.

Here, we used functional near-infrared spectroscopy (fNIRS; Chance et al. 1993) to investigate the neural correlates

of the SNARC effect. Similar to functional magnetic resonance imaging (fMRI), fNIRS monitors hemodynamic changes in the cerebral cortex (see Cutini et al. 2012, for a review); however, unlike the blood-oxygen-level-dependent (BOLD) signal of fMRI, which is gathered from the paramagnetic properties of deoxyhemoglobin (HbR), fNIRS is based on the intrinsic optical absorption of blood. As a result, fNIRS can simultaneously record the variations of HbR, oxygenated hemoglobin (HbO), and total hemoglobin (HbT) concentrations with a much higher temporal resolution, thereby potentially providing a richer picture of cortical hemodynamics compared with fMRI (see, e.g., Cutini et al. 2012, Scarpa et al. 2011; Brigadoi et al. 2012; Szűcs et al. 2012). Furthermore, fNIRS imposes negligible physical constraints on participants, and its tolerance to movement artifacts with respect to fMRI might be regarded as a further added value in the hunt for the SNARC effect. Finally, recent studies (Dresler et al. 2009; Richter et al. 2009) have shown that hemodynamic activity in the parietal cortex during the execution of numerical tasks can be reliably detected using fNIRS.

Hemodynamic activity of human parietal cortex was recorded during a standard magnitude comparison task with Arabic numerals, in which participants indicated via button-press whether single digits in the 1–9 range were greater or smaller than the reference number 5 (Fig. 1*a*). In SNARC-compatible trials, left-hand responses were given to small numbers (<5) and right-hand responses to large numbers (>5). In SNARC-incompatible trials, the mapping was reversed. This task allowed us to assess both SNARC and numerical distance effects (Fig. 1*b*). The latter indexes slower RTs for numbers close to the reference (at a distance of 1 or 2 units, i.e., 3, 4, 6, and 7) than for more distant numbers (at a distance of 3 or 4 units, i.e., 1, 2, 8, and 9) and provides a signature of magnitude processing, both behaviorally (Moyer and Landauer 1967) and neurally (Pinel et al. 2001).

Based on the hypothesis that the SNARC effect taps the spatial nature of a semantic representation of number magnitude (Dehaene et al. 1993; Zorzi et al. 2012), we predicted that the hemodynamic correlate of the SNARC effect would be found in the same regions supporting the representation of numerical magnitude, that is, in bilateral hIPS. More specifically, the cortical regions that show a modulation by numerical distance should also be modulated by SNARC compatibility.

To foreshadow the present set of results, we found a hemodynamic signature of the SNARC effect in the bilateral hIPS, at the same site that was modulated by numerical distance. Our findings point to number semantics as cognitive locus of number–space interactions, thereby revealing the intrinsic spatial nature of numerical magnitude representation. We also found an involvement of the left ANG, which is consistent with the mediating role of verbal/cultural factors in shaping the interaction between numbers and space.

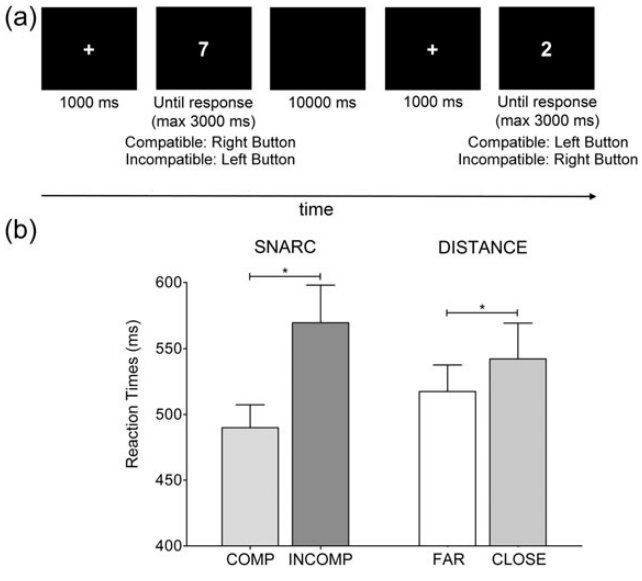

Figure 1. Experimental paradigm and behavioral data. (*a*) Schematic illustration of the experimental paradigm. (*b*) Bar graphs (mean and SD) of the behavioral SNARC (left) and distance effect (right).

Materials and Methods

Participants

Twelve healthy volunteers ($n = 12$, 27.8 years ± 4.5, 2 females) participated in the study after giving their written informed consent. All subjects were right-handed according to the Edinburgh Handedness Inventory (Oldfield 1971). The study was approved by the local ethics committee. All participants had normal or corrected to normal vision, were neurologically intact, and none of them were under medical treatment.

Stimuli, Procedure, and Behavioral Data Analysis

The experiment was conducted in a sound-attenuated, dimly lit room and was controlled by E-prime software (Psychology Software Tools Inc., Pittsburgh, PA, USA). The stimuli were white (40 cd/m^2) Arabic digits with a vertical side of 1.86° and a horizontal side of 0.91° of visual angle at a distance of 60 cm, which were displayed on a black (7 cd/m^2) background on a LCD monitor. A schematic illustration of the trial events is shown in Figure 1*a*. Each trial started with the presentation of a fixation cross at the center of the screen for 1 s. The fixation cross was then replaced by a digit from 1 to 9 (except 5, used as reference), which remained on screen until response (with a time limit of 3 s). After response, there was an interval with a blank screen for 10 s before the beginning of the next trial. Participants were instructed to maintain their gaze at fixation and to respond fast and accurately by pressing 1 of 2 buttons using the index finger of the right or the left hand, respectively. Participants performed 3 min of practice before starting the experiment. The latter had 160 trials divided in 2 blocks (80 compatible and 80 incompatible trials). In SNARC-incompatible trials, participants responded to numbers larger than 5 by pressing the left-sided button, whereas they pressed the right-sided button for numbers smaller than 5. This mapping was reversed in SNARC-compatible trials. Block order was counterbalanced across subjects. Numbers were randomly selected within each block, with 10 repetitions of each number.

fNIRS Instrumentation

The recording optical unit was a multichannel frequency-domain NIR spectrometer (ISS Imagent™, Champaign, IL), equipped with 32 laser diodes (16 emitting light at 690 nm, and 16 at 830 nm) modulated at 110.0 MHz. The diode-emitted light was conveyed to the subject's head by multimode core glass optical fibers (heretofore, sources; OFS Furukawa LOWOH series fibers, 0.37 of numerical aperture) with a length of 250 cm and a core diameter of 400 μm. Light that scattered through the brain tissue was carried by detector optical fiber bundles (diameter 3 mm) to 4 photomultiplier tubes (PMTs; R928 Hamamatsu Photonics). The PMTs were modulated at 110.005 MHz, generating a 5.0 kHz heterodyning (cross-correlation) frequency. To separate the light as a function of source location, the sources time-shared the 4

parallel PMTs via an electronic multiplexing device. Only 2 sources (1 per hemisphere) were synchronously ($t = 4$ ms) active (i.e., emitting light) resulting in a final sampling period of 128 ms ($f = 10^3/128 = 7.8125$ Hz), after a dual-period averaging.

fNIRS DPF Correction

Following detection and consequent amplification by the PMTs, the optical signal was converted into temporal variations of HbO and HbR (Cutini et al. 2008), where were subsequently age-corrected for the differential pathlength factor (DPF; Cope and Delpy 1988), which is sensitive to age differences (Schroeter et al. 2003, 2007), using the following equations (Duncan et al. 1996):

$$\mathrm{DPF}^{\mathrm{Hb0}} = 5.13 + 0.07 * (\mathrm{age}^{0.81}) \quad (1)$$
$$\mathrm{DPF}^{\mathrm{HbR}} = 4.67 + 0.062 * (\mathrm{age}^{0.877}) \quad (2)$$

Probe Placement

A single-distance probe arrangement aimed at maximizing the number of HbO–HbR measurement sites was adopted. Each source location (see Fig. 2 and SI Fig. 1) comprised 2 source optical fibers, one for each wavelength. The distance between each source/detector pair (hereafter, channel) was L = 35 mm, to equate the channels for optical penetration depth (~20 mm) into the cortical tissue (Franceschini et al. 2000). The probe configuration provided 20 channels, each measuring both HbO and HbR. Sources and detectors were held in place on the scalp using a custom-made head-mount system provided with velcro straps. The optodes were positioned using a probe placement method (Cutini, Scatturin et al. 2011) based on a physical model of the head surface of ICBM152 (Mazziotta et al. 2001) (the standard brain template in neuroimaging studies) and a 3D digitizing system (BrainSight™, Rogue Research). This method was used to find the optimal placement of the fNIRS probes in relation to the cerebral regions to be investigated that allowed to place the holder in a reproducible way across participants. This yielded a set of 10-20/10-10 reference points (Pz, PO3/4, and PO7/8) to place the probes on the bilateral posterior parietal cortex (PPC), the temporoparietal junction (TPJ), and the superior temporal gyrus (STG).

The probe arrangement was designed so that the recording sites (Fig. 2) included the target regions of interest, that is the hIPS, the ANG, and the posterior superior parietal lobule, defined according the stereotactic coordinates of Dehaene et al.'s (2003) meta-analysis; more details of the probe placement procedure are provided in SI *text* and SI Figure 1. Given that the coordinates of hIPS in Dehaene et al. (2003) (hereafter, hIPS-1) conflate the results obtained from markedly different paradigms and tasks, we also recorded the hemodynamic activity from a different zone of hIPS (hereafter, hIPS-2), highlighted by recent fMRI adaptation studies as a core region for magnitude representation (Piazza et al. 2004, 2007) (see SI *Text* and SI Fig. 2). Notably, the precision achieved with the probe placement procedure is comparable to that obtained with other methods (Okamoto et al. 2004; Okamoto and Dan 2005; Singh et al. 2005) and can yield a worst-case average error within the spatial resolution of the present fNIRS setup (Firbank et al. 1998).

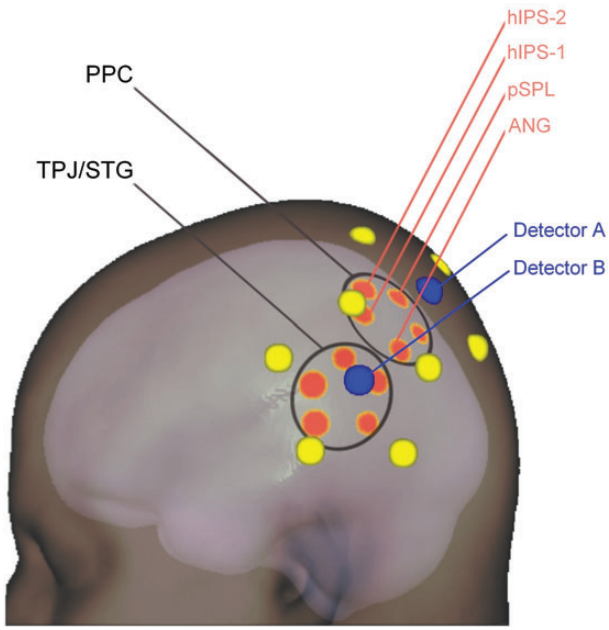

Figure 2. fNIRS recording sites superimposed on the ICBM152 template brain with the head in transparency. The 2 black ellipses describe the channels contained in the posterior parietal cortex (PPC) and the temporoparietal junction/superior temporal gyrus (TPJ/STG) macroregions. The yellow and blue circles correspond to the position of sources and detectors on the head surface, respectively. The red circles with yellow border correspond to the position of the channels on the cerebral cortex. The channels over the regions of interest are indicated with the red lines (hIPS, horizontal intraparietal sulcus; pSPL, posterior superior parietal lobule; ANG, angular gyrus; see Methods sections for further details).

fNIRS Signal Processing

Below we describe a series of operations, which were performed in both macroregion and channel-by-channel analyses. Individual hemodynamic responses were segmented into 11 s trials starting from 1 s before the stimulus onset to 10 s after. Each trial was zero-mean corrected by subtracting the mean intensity of the optical signal recorded during the 11 s period, to reduce the effect of low-frequency physiological noise when averaging the trials. The amplitude range (i.e., the difference between the maximum and minimum values) of each trial was calculated to remove artifacts: any trial with an amplitude range greater than the mean range ± 2.5 SDs in the specific experimental condition was considered as an outlier and then discarded. Subsequently, trials of the same condition were averaged. Channels with excessively noisy data (i.e., SD > 1600 nM, <5%) were discarded from the analysis.

The averaged hemodynamic response was smoothed with a Savitzky–Golay filter (Savitzky and Golay 1964), with polynomial order equal to 3 and frame size equal to 4 s, and it was baseline-corrected by subtracting from the overall hemodynamic response the mean intensity of the signal in the time interval between 1 s before and 1 s after the onset. For each channel, mean HbO and HbR concentrations were computed across a time window spanning the interval between 4 s and 8 s after trial onset. Peak latency was the time at which HbO reached its maximum value, and HbR reached its minimum value during the trial. Repeating these operations for each participant allowed us to generate distinct optical maps, one for HbO and another for HbR, for each experimental condition.

Macroregion Analysis

After performing the operations described in the "fNIRS signal processing" section (for each participant, condition, and channel), we divided the channels in 2 macroregions (Fig. 2): the PPC, including the channels surrounding detectors A and C, and the TPJ/STG, including the channels surrounding detectors B and D (A-B and C-D: left and right hemisphere, respectively). The mean hemodynamic activity in the 2 anatomical groups was pooled and submitted to repeated measures ANOVAs. Given that HbR did not reveal any significant activation, no further analysis was performed for such concentration. As an estimate of cerebral blood volume, one could use HbT concentration (Culver et al. 2005) (HbO + HbR). However, given that the HbR did not show a consistent event-related hemodynamic response (i.e., no channel resulted significantly activated in the macroregion analysis), we investigated only HbO concentration in the channel-by channel analysis.

Channel-by-Channel Analysis

The channel-by-channel analysis of HbO activity was restricted to the parietal lobe (i.e., PPC channels). Before performing the operations

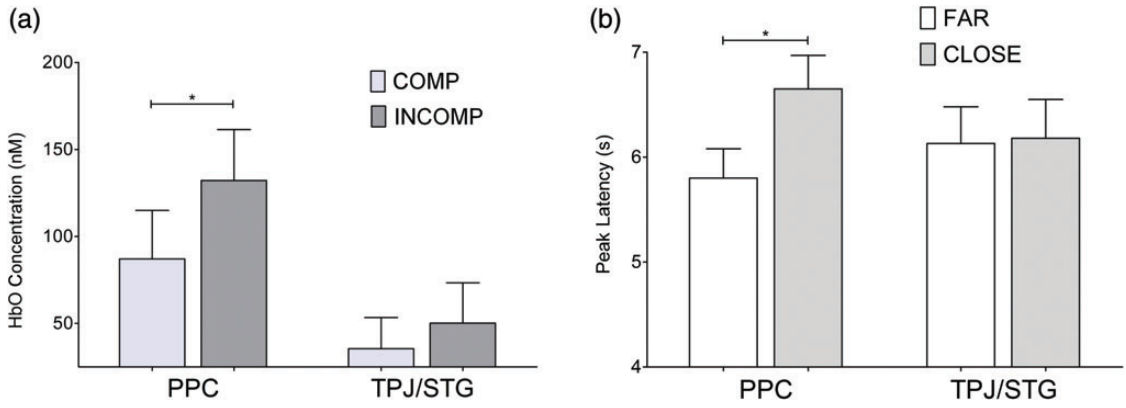

Figure 3. Macroregion analysis. Hemodynamic signatures of SNARC and distance effects were found in PPC but not in TPJ/STG. (*a*) SNARC compatibility modulated HbO amplitude. (*b*) Numerical distance modulated HbO peak latency. Values are pooled across hemispheres. Error bars represent mean standard error.

described in the "fNIRS signal processing" section, a technique based on principal component analysis (PCA) optimized for fNIRS (Virtanen et al. 2009) was applied to raw data to exclude the influence of global physiological activity from the fNIRS signal that could potentially bias the results (Franceschini et al. 2006). As 1) global physiological trends are presents in all channels (both HbO and HbR, with an opposite sign) and 2) PCA ability to identify a global physiological component improves with a high number of channels, the time series of all the 20 channels was considered. Furthermore, given that neither SNARC-compatibility nor numerical distance effect significantly affected TPJ/STG channels (in terms of amplitude or peak latency), their inclusion in PCA allowed to eliminate the global physiological effect, while preserving as much as possible the task-related hemodynamic response. To eliminate very slow drifts (<0.01 Hz), the raw time series of each channel was first high-pass filtered by subtracting the signal obtained with a third-order Savitsky–Golay filter with a window size of 60 s. Subsequently, PCA was applied and a coefficient of spatial uniformity (CSU) was computed for each obtained component. The CSU for a component k was defined as CSU $(k) = |w_k/\sigma_k|$, where w_k and σ_k are, respectively, the mean and standard deviation of the elements of the eigenvector of that component. A large value of CSU can be interpreted to identify the global physiological effect, so the component with the largest CSU was subtracted from each time series (Virtanen et al. 2009). The component with the largest CSU typically included hemodynamic fluctuations caused by heartbeat, respiration, and Mayer waves (Franceschini et al. 2006; Sassaroli et al. 2012). After PCA application, the series of operations described on "fNIRS signal processing" section were repeated for each participant and condition, to create an individual optical map of HbO concentration in PPC channels for every condition. Similarly, we created an individual optical map of HbO peak latency in PPC channels for every condition and subject. The SNARC and distance effects in PPC channels were investigated with a series of one-tailed paired *t*-tests; both peak latency and amplitude of hemodynamic responses were compared (SNARC: incompatible vs. compatible; distance: close vs. far). The difference in peak latencies was evaluated by using cross-correlation analysis: the output resulted in the time-lag value providing the highest correlation between the hemodynamic responses observed in the 2 conditions. A trimming procedure was performed on time-lag values: outliers (5% threshold) were discarded and replaced by mean individual time-lag values. All the *t*-test series were corrected for multiple comparisons using a false discovery rate (FDR; Singh and Dan 2006) with $q = 0.05$.

The significant t values were converted into z scores to create z-maps. The z score of each channel was mapped onto an overlay map (1-mm^3 voxel size) at the correspondent midpoint expressed in MNI coordinates, using the Nifti toolbox (Neuroimaging Informatics Technology Initiative, http://www.nifti.nimh.nih.gov). A Gaussian blurring filter (SD = 10 mm) was then applied to the overlay map to approximate the area covered by each channel (Cutini et al. 2008, Cutini, Scarpa et al. 2011). Finally, the resulting z-map was overlaid onto the reference brain using MRicron software (http://www.mccauslandcenter.sc.edu/mricro/mricron/index.html). All the computations were performed using custom-made code in Matlab (ver. R2010a, The Mathworks Inc., Natick, Massachusetts, USA).

Results

Individual mean RTs were calculated for each condition (compatible, incompatible, far, and close), discarding values exceeding the respective mean ± 2.5 SDs. SNARC and distance effects were analyzed with 2 separate ANOVAs. The ANOVAs on RTs revealed, as expected, a significant effect of SNARC ($F_{1,11} = 14.67$, $P = 0.003$) and distance ($F_{1,11} = 22.74$, $P = 0.001$) (Fig. 1*b*).

The hemodynamic response was analyzed both in terms of response amplitude and peak latency. We first divided the channels in 2 macroregions for each hemisphere, that is, PPC and TPJ/STG (Fig. 2), and pooled their activities. The analyses, in addition to region (PPC, TPJ/STG) and hemisphere (left, right), had either SNARC-compatibility or distance as factors. All observed modulations were restricted to HbO concentration (see Methods section for further details). The PPC showed higher response amplitude than TPJ/STG ($F_{1,11} = 10.35$, $P = 0.008$) and it was modulated by SNARC-compatibility: incompatible trials elicited larger hemodynamic responses relative to compatible trials (2-way interaction: $F_{1,11} = 6.56$, $P = 0.044$; Fig. 3*a*). The analysis with distance revealed only a higher activity of the PPC ($F_{1,11} = 9.31$, $P = 0.011$; all the other Ps > 0.15). Conversely, the peak latency of the PPC (but not of TPJ/STG) was modulated by numerical distance (2-way interaction: $F_{1,11} = 10.23$, $P = 0.008$), with a delay for close numbers with respect to far numbers (Fig. 3*b*). SNARC-compatibility had no effect on peak latency (Ps > 0.16).

Having established that PPC activity is modulated by the SNARC effect, we performed a channel-by-channel analysis of HbO activity in this region to precisely locate the neural locus of the SNARC effect. A version of PCA optimized for fNIRS data was performed to exclude the influence of global physiological activity from hemodynamic data (see Methods section). Two series of paired *t*-tests [corrected for multiple comparisons using a FDR with $q = 0.05$ (Singh and Dan

2006)] were performed, 1 for peak latencies and 1 for the amplitude of hemodynamic responses. Numerical distance bilaterally modulated the peak latency of hIPS-1/hIPS-2 (Table 1 provides the statistical values referring to the active subset of the investigated regions), with a delay for close numbers with respect to far numbers, but it did not influence the amplitude of hemodynamic response ($Ps > 0.19$). Conversely, the SNARC effect strongly modulated the bilateral response amplitude of hIPS (z-maxima in left hIPS-2; $z = 3.02$, $P = 0.013$) and left ANG: hemodynamic activity in these regions was larger during incompatible trials than compatible trials, but there were no effects on peak latency ($Ps > 0.15$) (Fig. 4*a–d*).

We performed additional analyses on the bilateral activity of hIPS to rule out the hypothesis that the stronger activation of hIPS during incompatible trials would reflect increased difficulty of response selection (Göbel et al. 2004; Shuman and Kanwisher 2004), as indexed by slower RTs. We selected the 4 channels of interest (left and right hIPS-1 and hIPS-2), and, for each participant, we calculated dHbO as the difference between hemodynamic activity for incompatible trials and compatible trials. Likewise, we calculated dRT as the difference between RTs in incompatible and compatible trials. Analysis of dHbO with hemisphere (left and right) and channel (hIPS-1 and hIPS-2) as factors and dRT as covariate revealed a main effect of channel ($F_{1,10} = 9.61$; $P = 0.011$) and a significant interaction between channel and dRT ($F_{1,10} = 9.68$; $P = 0.011$; other main effects and interactions nonsignificant ($Ps > 0.12$). The interaction between channel and dRT was further explored with a partial correlation analysis (a stringent analysis performed by correlating each channel with dRT while controlling for the respective nearest channel). The hIPS-1 was correlated with dRT (left: $R = 0.522$, $P = 0.05$; right: $R = 0.517$, $P = 0.052$), whereas hIPS-2 was not (left: $R = -0.109$; right: $R = -0.175$, $Ps > 0.28$): the difference between correlations was significant (Hotelling-Williams tests: left sites, $T_9 = 2.33$, $P = 0.022$; right sites, $T_9 = 3.09$, $P = 0.006$).

Table 1.
Regions of the PPC modulated by SNARC and/or distance effect

MNI coordinates			Anatomical information			Statistical results (z scores)	
x	*y*	*z*	Hemisphere	Region	BA	SNARC	Distance
−33	−54	65	left	hIPS-2	7/40	3.02	2.25
34	−53	65	right	hIPS-2	7/40	2.12	2.71
−45	−53	55	left	hIPS-1	7/40	2.39	n.s.
44	−53	57	right	hIPS-1	7/40	n.s.	2.33
−45	−68	41	left	ANG	39	2.06	n.s.

From left to right: MNI coordinates (*x*, *y*, and *z*), hemisphere, anatomical region, and Brodmann area (BA).
The last 2 columns show the *z* scores for the SNARC effect (amplitude modulation) and the distance effect (peak latency modulation).

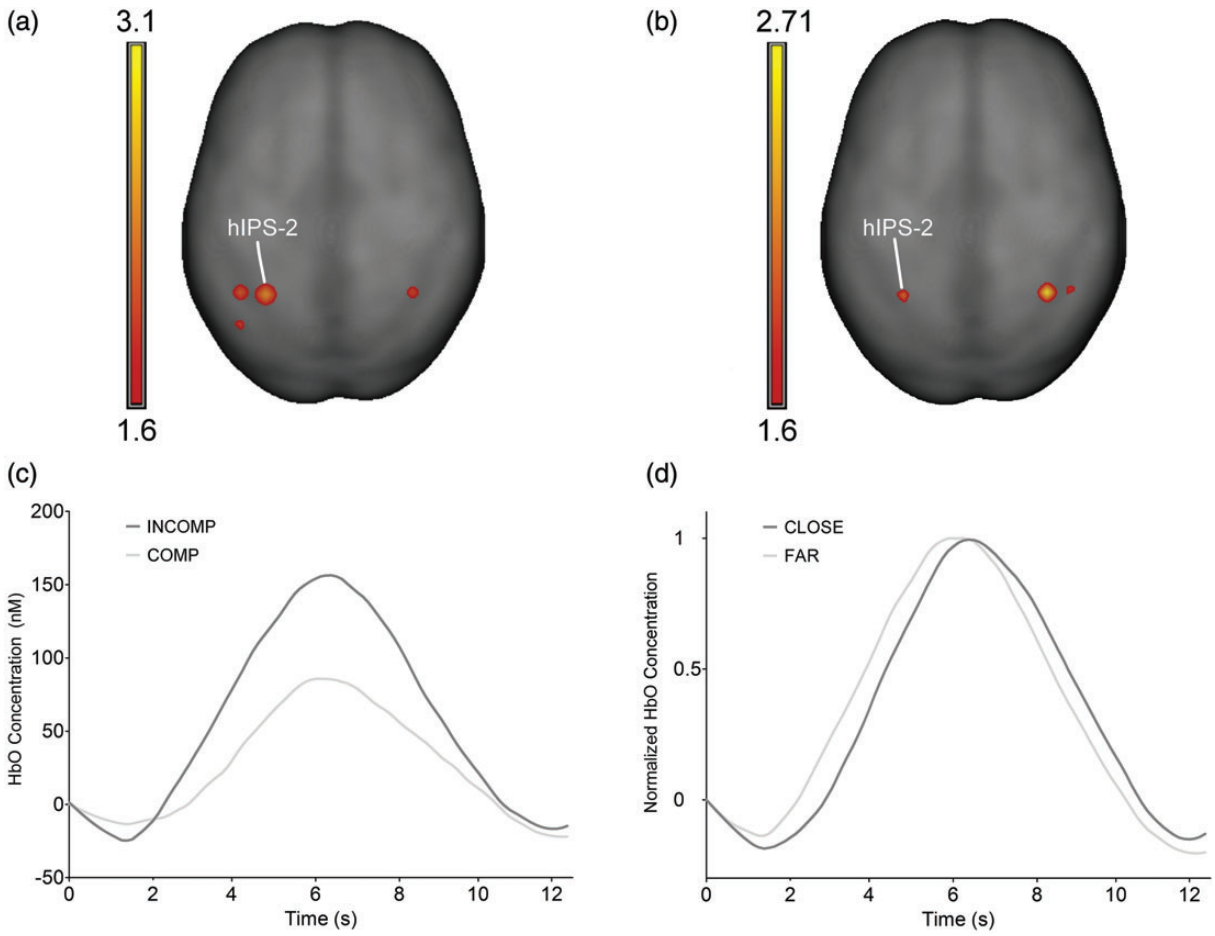

Figure 4. Channel-by-channel analysis. Neural correlates of SNARC effect (on HbO amplitude) and distance effect (on HbO peak latency) in the PPC. Statistical (*z*) maps (*a* and *b*) and hemodynamic response profiles of hIPS-2 (*c* and *d*) in incompatible versus compatible trials and in close versus far trials.

This pattern suggests that the SNARC modulation of hIPS-2 activity is not driven by response selection/task difficulty. Most importantly, the higher correlation between dHbO and dRT in hIPS-1 was not related to a generally stronger hemodynamic modulation, because the largest hemodynamic SNARC effect was observed in hIPS-2, despite its lack of correlation with its behavioral counterpart.

Discussion

We found a robust hemodynamic signature of the SNARC effect in 2 different parietal areas that are routinely involved in number processing tasks, the bilateral hIPS and the left ANG. The modulation of the bilateral hIPS, the core region for numerical magnitude representation (Piazza et al. 2004), is consistent with an account of the effect that hinges on the inherently spatial nature of number representation (i.e., a left-to-right oriented mental number line; Dehaene et al. 1993, 2003; Zorzi et al. 2002; Hubbard et al. 2005; Zorzi et al., 2012). Crucially, the peak latency of the hemodynamic response in the same region was modulated by numerical distance, thereby providing a clear and unambiguous signature of numerical magnitude activation. This is consistent with recent neuropsychological findings showing abnormal SNARC and distance effects in right hemisphere damaged patients with neglect during number comparison (Zorzi et al. 2012). Interestingly, rTMS over the bilateral PPC has been shown to reduce the SNARC effect during a parity judgment task (Rusconi et al. 2007).

However, IPS—more broadly defined—is also activated in non-numerical tasks requiring left versus right key-presses (Jiang and Kanwisher 2003), and its activity is correlated with response selection difficulty (Shuman and Kanwisher 2004), as indexed by RTs. It has been argued that IPS activity during magnitude comparison would reflect response selection rather than access to numerical magnitude (Göbel et al. 2004). Though the specific role of hIPS in the representation of numerical magnitude has been unambiguously revealed by fMRI adaptation studies (Piazza et al. 2004, 2007), as well as by multivoxel pattern recognition analyses (Eger et al. 2009; Zorzi et al. 2011), it is important to rule out a response selection account of the HbO modulation found in the present study. In this regard, the results of our ANCOVA and partial correlation analyses show that the influence of response selection is not ubiquitous but it dissociates in 2 distinct portions of the IPS. Indeed, activity in hIPS-2 did not correlate with RTs (unlike hIPS-1). Note that the coordinates of our hIPS-2 region were close to those reported in fMRI number adaptation studies (SI Fig. 2). Together with the finding that activity in the same intraparietal region was temporally modulated by numerical distance, the present results point to a semantic locus of the number–space interaction and can be hardly reconciled with accounts of the SNARC effect that are exclusively concerned with the response selection stage or claim that it does not imply the mental number line (Gevers, Verguts et al. 2006; Santens and Gevers 2008; Fias et al. 2011). Our results are consistent with a recent computational model (Chen and Verguts 2010) assuming that the environmental correlation between symbolic numbers and physical space must leave a neural signature that is at the heart of number–space interactions.

One recent alternative account of the SNARC effect, however, postulates that numbers might be associated with multiple spatial codes and that, depending on the task, these codes have a verbal or visuospatial basis (van Dijck et al. 2009; Gevers et al. 2010). Consistent with this view is the finding that the SNARC effect in the parity-judgment task disappeared under verbal but not under spatial working memory load, whereas the opposite was found for the SNARC effect in the magnitude comparison task (van Dijck et al. 2009). In the same vein, holding visuospatial information in memory was shown to prevent the occurrence of the SNARC effect (Herrera et al. 2008). Interestingly, we found a signature of the SNARC effect also in the left ANG, a region that is held to be mainly responsible for the verbal/linguistic aspects of number processing (Dehaene et al. 2003), suggesting that language might also play a role in this effect. This is also consistent with the hypothesis that verbal–spatial coding coexists with visuospatial coding of numbers (Gevers et al. 2010). This dovetails nicely with the finding that the SNARC effect is shaped by culture (Dehaene et al. 1993). Indeed, the spatial orientation of the number line (i.e., left-to-right or right-to-left) is modulated by reading habits, as revealed by studies that directly compared participants who read from left to right or from right to left (Shaki et al. 2009).

In light of the extensive behavioral and neuropsychological investigation of number–space interactions, one might wonder why no previous study to date has revealed the neural correlates of the SNARC effect. One possibility to consider is a lack of positive findings with fMRI. In this regard, it is worth mentioning that we obtained significant results in the analysis of HbO concentration only, whereas HbR (which is what the BOLD fMRI signal represents) did not show a significant modulation of the hemodynamic response. However, the different results observed with HbO and HBR are probably linked to the different sensitivity of fNIRS to the 2 chromophores. Given that HbO response is markedly stronger than that of HbR (Watanabe et al. 1996; Sato et al. 2004), the high source-detector distance might have played against the possibility to record a reliable HbR response. A more critical difference between fNIRS and fMRI might be found in the standard scanning setup. For instance, the supine body position inside the fMRI scanner might interfere with number–space interactions by eliciting a different spatial frame of reference, thereby diluting the SNARC effect. A recent study investigating the effect of numerical cues on the orienting of spatial attention yielded significant behavioral effects outside the fMRI scanner, but not inside it (Goffaux et al. 2010). Moreover, the recent finding that fMRI scanner noise leads participants to increase cognitive control (Hommel et al. 2012), thereby reducing the impact of the competing response code, suggests another possible factor that might dilute the SNARC effect inside the scanner. A combined fMRI–fNIRS study would be ideal to shed light on this issue.

In conclusion, our findings point to a semantic locus of the interaction between numbers and space, thereby refuting the claim that the SNARC effect is entirely confined to the response selection stage (Keus and Schwarz 2005; Keus et al. 2005) and disproving theories that dispense with a spatial representation of numbers (Proctor and Cho 2006; Santens and Gevers 2008). Nonetheless, the SNARC effect remains an intriguing and multifaceted phenomenon, because it is the result of a complex interaction between numbers, space, and culture.

Authors Contributions

S.C. and M.Z. designed research. S.C., F.S., and P.S. performed research. S.C. and F.S. analyzed data. M.Z. and R.D.A. contributed to data analysis and interpretation. S.C., M.Z., F.S., and R.D.A. wrote the manuscript.

Funding

This study was supported by grants from Cariparo Foundation (Progetti di Eccellenza 2007), Italian Ministry of Education and Research (PRIN 2008) and European Research Council (# 210922) to M.Z.

Note

Conflict of Interest: None declared.

References

Brigadoi S, Cutini S, Scarpa F, Scatturin P, Dell'Acqua R. 2012. Exploring the role of primary and supplementary motor areas in simple motor tasks with fNIRS. Cogn process. 13:97–101.

Castronovo J, Seron X. 2007. Semantic numerical representation in blind subjects: the role of vision in the spatial format of the mental number line. Q J Exp Psychol (2006). 60:101–119.

Chance B, Zhuang Z, Unah C, Alter C, Lipton L. 1993. Cognition-activated low-frequency modulation of light absorption in human brain. Proc Natl Acad Sci USA. 90:3770–3774.

Chen Q, Verguts T. 2010. Beyond the mental number line: a neural network model of number-space interactions. Cogn Psychol. 60:218–240.

Chochon F, Cohen L, van De Moortele PF, Dehaene S. 1999. Differential contributions of the left and right inferior parietal lobules to number processing. J Cogn Neurosci. 11:617–630.

Cope M, Delpy DT. 1988. System for long-term measurement of cerebral blood and tissue oxygenation on newborn infants by near infra-red transillumination. Med Biol Eng Comput. 26:289–294.

Culver JP, Siegel AM, Franceschini MA, Mandeville JB, Boas DA. 2005. Evidence that cerebral blood volume can provide brain activation maps with better spatial resolution than deoxygenated hemoglobin. Neuroimage. 27:947–959.

Cutini S, Basso Moro S, Bisconti S. 2012. Functional near infrared optical imaging in cognitive neuroscience: an introductory review. J Near Infrared Spectrosc. 20:75–92.

Cutini S, Scarpa F, Scatturin P, Jolicœur P, Pluchino P, Zorzi M, Dell'Acqua R. 2011. A hemodynamic correlate of lateralized visual short-term memories. Neuropsychologia. 49:1611–21.

Cutini S, Scatturin P, Menon E, Bisiacchi PS, Gamberini L, Zorzi M, Dell'Acqua R. 2008. Selective activation of the superior frontal gyrus in task-switching: an event-related fNIRS study. Neuroimage. 42:945–955.

Cutini S, Scatturin P, Zorzi M. 2011. A new method based on ICBM152 head surface for probe placement in multichannel fNIRS. Neuroimage. 54:919–927.

Dehaene S, Bossini S, Giraux P. 1993. The mental representation of parity and number magnitude. J Exp Psychol Gen. 122:371–396.

Dehaene S, Piazza M, Pinel P, Cohen L. 2003. Three parietal circuits for number processing. Cogn Neuropsychol. 20:487–506.

Dresler T, Obersteiner A, Schecklmann M, Vogel AC, Ehlis A-C, Richter MM, Plichta MM, Reiss K, Pekrun R, Fallgatter AJ. 2009. Arithmetic tasks in different formats and their influence on behavior and brain oxygenation as assessed with near-infrared spectroscopy (NIRS): a study involving primary and secondary school children. J Neural Transm. 116:1689–700.

Duncan A, Meek J, Clemence M, Elwell C, Fallon P, Tyszczuk L, Cope M, Delpy D. 1996. Measurement of cranial optical path length as a function of age using phase resolved near infrared spectroscopy. Pediatr Res. 39:889–894.

Eger E, Michel V, Thirion B, Amadon A, Dehaene S, Kleinschmidt A. 2009. Deciphering cortical number coding from human brain activity patterns. Curr Biol. 19:1608–1615.

Eger E, Sterzer P, Russ MO, Giraud A-L, Kleinschmidt A. 2003. A supramodal number representation in human intraparietal cortex. Neuron. 37:719–725.

Fias W, Brysbaert M, Geypens F, d' Ydewalle G. 1996. The importance of magnitude information in numerical processing: evidence from the SNARC effect. Math Cogn. 2:95–110.

Fias W, van Dijck J-P, Gevers W. 2011. How number is associated with space? The role of working memory. In: Dehaene S, Brannon EM, editors. Space, Time and Number in the Brain—Searching for Evolutionary Foundations of Mathematical Thought. Amsterdam: Academic Press (Attention and performance). p. 133–148.

Firbank M, Okada E, Delpy DT. 1998. A theoretical study of the signal contribution of regions of the adult head to near-infrared spectroscopy studies of visual evoked responses. Neuroimage. 8:69–78.

Franceschini MA, Joseph DK, Huppert TJ, Diamond SG, Boas DA. 2006. Diffuse optical imaging of the whole head. J Biomed Opt. 11:054007.

Franceschini MA, Toronov V, Filiaci M, Gratton E, Fantini S. 2000. On-line optical imaging of the human brain with 160-ms temporal resolution. Opt Express. 6:49–57.

Gevers W, Lammertyn J. 2005. The hunt for SNARC. Psychol Sci. 47:10–21.

Gevers W, Ratinckx E, De Baene W, Fias W. 2006. Further evidence that the SNARC effect is processed along a dual-route architecture. Exp Psychol. 53:58–68.

Gevers W, Santens S, Dhooge E, Chen Q, Van den Bossche L, Fias W, Verguts T. 2010. Verbal-spatial and visuospatial coding of number-space interactions. J Exp Psychol Gen. 139:180–190.

Gevers W, Verguts T, Reynvoet B, Caessens B, Fias W. 2006. Numbers and space: a computational model of the SNARC effect. J Exp Psychol Hum Percept Perform. 32:32–44.

Göbel SM, Johansen-Berg H, Behrens T, Rushworth MFS. 2004. Response-selection-related parietal activation during number comparison. J Cogn Neurosci. 16:1536–1551.

Göbel SM, Shaki S, Fischer MH. 2011. The cultural number line: a review of cultural and linguistic influences on the development of number processing. J Cross Cult Psychol. 42:543–565.

Goffaux V, Dormal G, Goebel R, Martin R, Schiltz C. 2010. The neuronal correlates of visuo-spatial attentional shifts induced by irrelevant numerical cues: an fMRI study. 16th Annual Meeting of the OHBM. Barcelona, Spain.

Herrera A, Macizo P, Semenza C. 2008. The role of working memory in the association between number magnitude and space. Acta psychol. 128:225–237.

Hommel B, Fischer R, Colzato LS, van den Wildenberg WPM, Cellini C. 2012. The effect of fMRI (noise) on cognitive control. J Exp Psychol Hum Percept Perform. 38:290–301.

Hubbard EM, Piazza M, Pinel P, Dehaene S. 2005. Interactions between number and space in parietal cortex. Nat Rev Neurosci. 6:435–448.

Jiang Y, Kanwisher N. 2003. Common neural substrates for response selection across modalities and mapping paradigms. J Cogn Neurosci. 15:1080–1094.

Keus IM, Jenks KM, Schwarz W. 2005. Psychophysiological evidence that the SNARC effect has its functional locus in a response selection stage. Cogn Brain Res. 24:48–56.

Keus IM, Schwarz W. 2005. Searching for the functional locus of the SNARC effect: evidence for a response-related origin. Mem Cognit. 33:681–695.

Mazziotta J, Toga A, Evans A, Fox P, Lancaster J, Zilles K, Woods R, Paus T, Simpson G, Pike B et al. 2001. A probabilistic atlas and reference system for the human brain: International Consortium for Brain Mapping (ICBM). Philos Trans R Soc Lond B Biol Sci. 356:1293–1322.

Moyer RS, Landauer TK. 1967. Time required for judgements of numerical inequality. Nature. 215:1519–1520.

Nuerk H-C, Wood G, Willmes K. 2005. The Universal SNARC Effect. Exp Psychol. 52:187–194.
Okamoto M, Dan I. 2005. Automated cortical projection of head-surface locations for transcranial functional brain mapping. Neuroimage. 26:18–28.
Okamoto M, Dan H, Sakamoto K, Takeo K, Shimizu K, Kohno S, Oda I, Isobe S, Suzuki T, Kohyama K et al. 2004. Three-dimensional probabilistic anatomical cranio-cerebral correlation via the international 10–20 system oriented for transcranial functional brain mapping. Neuroimage. 21:99–111.
Oldfield RC. 1971. The assessment and analysis of handedness: the Edinburgh inventory. Neuropsychologia. 9:97–113.
Piazza M, Izard V, Pinel P, Le Bihan D, Dehaene S. 2004. Tuning curves for approximate numerosity in the human intraparietal sulcus. Neuron. 44:547–555.
Piazza M, Pinel P, Le Bihan D, Dehaene S. 2007. A magnitude code common to numerosities and number symbols in human intraparietal cortex. Neuron. 53:293–305.
Pinel P, Dehaene S, Rivière D, LeBihan D. 2001. Modulation of parietal activation by semantic distance in a number comparison task. Neuroimage. 14:1013–1026.
Proctor RW, Cho YS. 2006. Polarity correspondence: a general principle for performance of speeded binary classification tasks. Psychol Bull. 132:416–442.
Richter MM, Zierhut KC, Dresler T, Plichta MM, Ehlis A-C, Reiss K, Pekrun R, Fallgatter AJ. 2009. Changes in cortical blood oxygenation during arithmetical tasks measured by near-infrared spectroscopy. J Neural Transm. 116:267–73.
Rusconi E, Turatto M, Umiltà CA. 2007. Two orienting mechanisms in posterior parietal lobule: an rTMS study of the Simon and SNARC effects. Cogn Neuropsychol. 24:373–392.
Santens S, Gevers W. 2008. The SNARC effect does not imply a mental number line. Cognition. 108:263–270.
Sassaroli A, Pierro M, Bergethon P, Fantini S. 2012. Low-frequency spontaneous oscillations of cerebral hemodynamics investigated with near-infrared spectroscopy: a review. IEEE J Sel Topics Quantum Electron. 18:1478–1492.
Sato H, Kiguchi M, Kawaguchi F, Maki A. 2004. Practicality of wavelength selection to improve signal-to-noise ratio in near-infrared spectroscopy. Neuroimage. 21:1554–1562.
Savitzky A, Golay MJE. 1964. Smoothing and differentiation of data by simplified least squares procedures. Anal Chem. 36: 1627–1639.
Schroeter ML, Cutini S, Wahl MM, Scheid R, Yves von Cramon D. 2007. Neurovascular coupling is impaired in cerebral microangiopathy—an event-related Stroop study. Neuroimage. 34:26–34.
Schroeter ML, Zysset S, Kruggel F, Cramon DYV. 2003. Age dependency of the hemodynamic response as measured by functional near-infrared spectroscopy. Neuroimage. 19: 555–564.
Shaki S, Fischer MH, Petrusic WM. 2009. Reading habits for both words and numbers contribute to the SNARC effect. Psychon Bull Rev. 16:328–331.
Shuman M, Kanwisher N. 2004. Numerical magnitude in the human parietal lobe; tests of representational generality and domain specificity. Neuron. 44:557–569.
Singh AK, Dan I. 2006. Exploring the false discovery rate in multichannel NIRS. Neuroimage. 33:542–549.
Singh AK, Okamoto M, Dan H, Jurcak V, Dan I. 2005. Spatial registration of multichannel multi-subject fNIRS data to MNI space without MRI. Neuroimage. 27:842–851.
Szűcs D, Killikelly C, Cutini S. 2012. Event-related near-infrared spectroscopy detects conflict in the motor cortex in a Stroop task. Brain Res. 1477:27–36.
Tang Y, Zhang W, Chen K, Feng S, Ji Y, Shen J, Reiman EM, Liu Y. 2006. Arithmetic processing in the brain shaped by cultures. Proc Natl Acad Sci USA. 103:10775–10780.
van Dijck J-P, Gevers W, Fias W. 2009. Numbers are associated with different types of spatial information depending on the task. Cognition. 113:248–253.
Virtanen J, Noponen T, Meriläinen P. 2009. Comparison of principal and independent component analysis in removing extracerebral interference from near-infrared spectroscopy signals. J Biomed Opt. 14:054032.
Watanabe E, Yamashita Y, Maki A, Ito Y, Koizumi H. 1996. Non-invasive functional mapping with multi-channel near infra-red spectroscopic topography in humans. Neurosci Lett. 205:41–44.
Zorzi M, Bonato M, Treccani B, Scalambrin G, Marenzi R, Priftis K. 2012. Neglect impairs explicit processing of the mental number line. Front Hum Neurosci. 6:125
Zorzi M, Di Bono MG, Fias W. 2011. Distinct representations of numerical and non-numerical order in the human intraparietal sulcus revealed by multivariate pattern recognition. Neuroimage. 56:674–680.
Zorzi M, Priftis K, Umiltà C. 2002. Brain damage: neglect disrupts the mental number line. Nature. 417:138–139.